J Mar Sci Technol (2016) 21:715–728
DOI 10.1007/s00773-016-0386-x

ORIGINAL ARTICLE

Experimental study on piston- and sloshing- mode moonpool resonances

Seung-Ho Yang[1] · Sang-Beom Lee[2] · Jung-Ho Park[2] · Seung-Yoon Han[2] · Young-Myung Choi[2] · Jitae Do[2] · Sun-Hong Kwon[2] · Bernard Molin[3]

Received: 6 July 2015 / Accepted: 16 April 2016 / Published online: 2 May 2016

Abstract An experimental study was performed on the piston- and sloshing-mode moonpool resonances of offshore structures. Two different geometries were considered to investigate the flow characteristics in a plain moonpool and a moonpool with a cofferdam. To examine the efficiency of a cofferdam for reducing the flow in a moonpool, three cofferdam geometries were tested. The plain moonpool presented violent flows as a result of the piston- and sloshing-mode resonances. However, the moonpool with the cofferdam introduced violent sloshing waves instead of the ascent and descent of the water column in the piston-mode moonpool resonance. Among three different cofferdam geometries, the model with a right triangle facing to the left on the top of the cofferdam was most effective in reducing the flow in the moonpool when compared with the other models.

Keywords Piston-mode · Sloshing-mode · Moonpool resonance · Cofferdam

1 Introduction

Despite a global recession over the last few years, the global economy is projected to grow based on an increase in worldwide economic activities and the expansion of trade. According to these trends, the oil and gas industry is reshaping its energy economy. With an increase in the need for offshore exploration, the number of offshore platforms has dramatically increased, and research and development around such offshore platforms has been actively conducted. One of the most representative floating offshore structures for oil and gas exploration is a drillship, and the demand for this is increasing compared with other offshore plants [1].

Since the mobility of a drillship is enabled by its propulsion system, it can move from one offshore field to another [2]. New emerging drillships are equipped with high capacity dynamic positioning systems. These devices make it possible to work in harsh environments, including the North Sea, up to a water depth of 10,000 ft [14].

When it comes to the design of floating offshore structures, such as drillships, the designers give priority to the safety of workers and security of the operation. Due to the high cost of chartering, any downtime caused by environmental factors must be reduced. Therefore, oil majors and charterers are keen to guarantee the desired operation time at an early design stage [6].

A drillship has an open area, called a "moonpool" in the center of the ship. The moonpool structure affects the working conditions, such as the operation of risers, and the lowering and recovery of subsea equipment [10]. Although a moonpool is very essential for this type of offshore structure, it affects the operation time and has some disadvantages in terms of the overall performance of the vessel.

One of the major factors that affects the operation time is a violent flow in the moonpool [13]. Many researchers have tried to reduce the flow in the moonpool. Experimental studies in this area were found in the following works [3–5, 9]. Although previous studies found interesting flow phenomena in a moonpool, they failed to provide

✉ Sun-Hong Kwon
shkwon@pusan.ac.kr

[1] Department of Naval Architecture and Ocean Engineering, Ulsan College, Ulsan, Korea

[2] Department of Naval Architecture and Ocean Engineering, Pusan National University, Busan, Korea

[3] École Centrale de Marseille and IRPHÉ, Marseille, France

drillship designers with fundamental solutions to reduce the flow in the moonpool. Furthermore, most of the offshore structures installed in the ocean are floating rather than fixed. They are exposed to waves which can approach from any direction. The draft also changes. Hence, moonpool designers should consider the wave direction, draft, and other considerable factors.

A better solution is to develop formulas or tools to predict the resonance frequency during the design stage instead of trying to reduce the wave elevation afterwards. It is well known that a moonpool can have two types of resonance modes: the piston-mode and sloshing-mode. Molin [8] derived analytic formulas to evaluate the moonpool resonance frequency based on potential theory. Yang et al. [11, 12] confirmed validity of Molin's analytic formula through experimental studies.

Purpose of this study is to investigate the flow characteristics in a moonpool for the piston and sloshing-modes through extensive model tests with various wave frequencies and wave headings. Furthermore, efficiency of different cofferdam geometries was tested to investigate whether the flow in the moonpool was reduced.

2 Experiments

Model tests were performed for the items listed below.

1. Piston-mode and sloshing-mode moonpool resonances in a plain moonpool.
2. Effect of a cofferdam in the moonpool on the piston-mode and sloshing-mode.
3. Effect of different incident wave directions on the water elevation inside the moonpool.
4. Influence of triangular structures installed on the top of a cofferdam at the water elevation inside the moonpool.

A schematic for the model test is shown in Fig. 1.

To verify the efficiency of a cofferdam which reduces the flow in the moonpool, geometries of three different cofferdams were tested: a rectangular shaped cofferdam and cofferdams with right triangular structure facing right and facing left. The dimensions of each cofferdam are shown in Fig. 2.

Principal dimensions of two-dimensional (2D) wave flumes are presented in Table 1. Figure 3 shows 2D wave flume at Pusan National University (PNU) and a potentiometer for measurements of the motion. Figure 4 shows 2D wave flume at Koje College and the same potentiometer. The test model was installed below the potentiometer. The locations of the wave gauges are shown in Fig. 5. Since the width of wave flume at PNU is 0.6 m, an oblique test could not be conducted; therefore, the oblique test was carried out in 2D wave flume at Koje College. As shown in Fig. 4, the width of the wave flume at Koje College is 2.0 m, much wider than that at PNU.

3 Models

Three types of models were tested. Model B was a test model without the cofferdam. Model Bc was with a rectangular-type cofferdam, Model Bc_tri was with a triangular structure on the top of the cofferdam. The main dimensions of each model are presented in Table 2. Main dimensions of Model B, Model Bc, and Model Bc_tri are the same. The model tests were conducted with drafts of 11

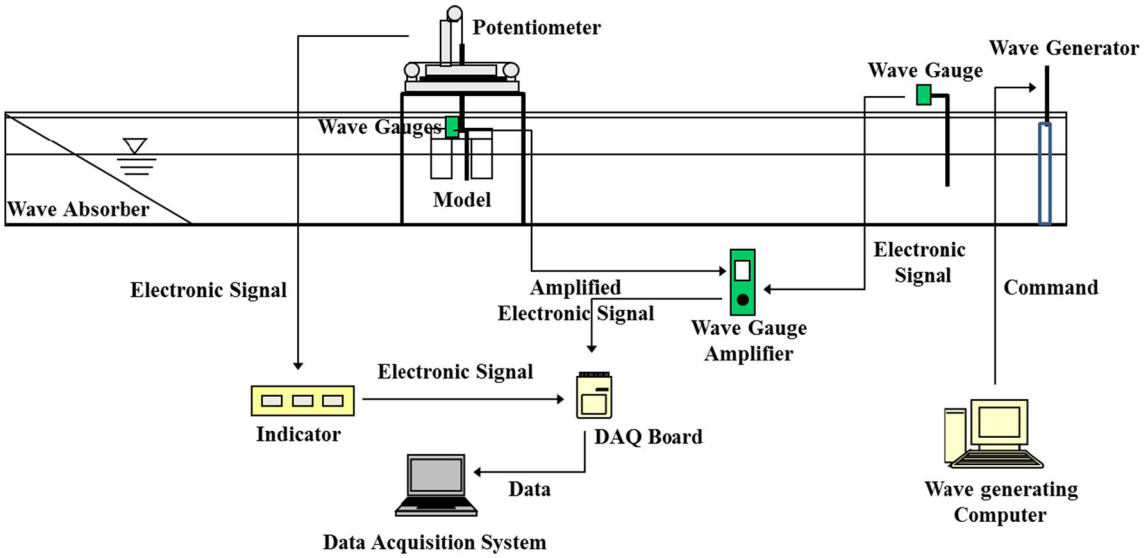

Fig. 1 Schematic for model test

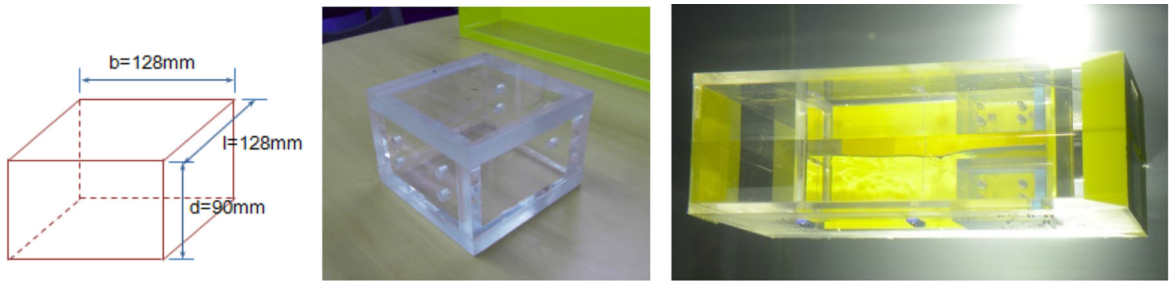

Rectangular type cofferdam (left: cofferdam only, right: cofferdam installed in the moonpool)

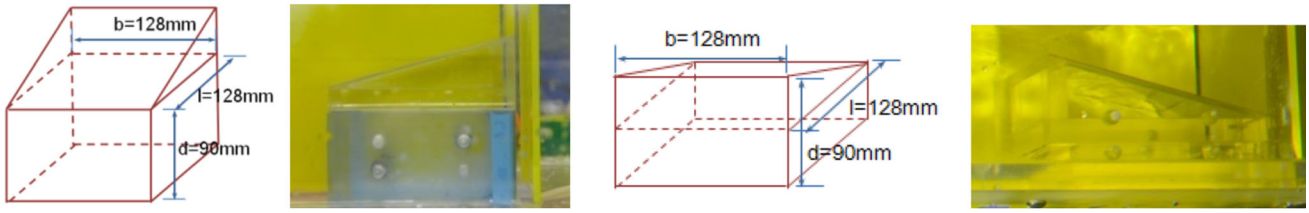

Cofferdam + triangular structure (left: right triangle facing left, right: right triangle facing right)

Fig. 2 Geometries of three different cofferdams

Table 1 Principal dimensions of 2D wave flumes

2D wave flume at PNU (m)		2D wave flume at Koje College (m)	
Length	31.2	Length	30.0
Breadth	0.6	Breadth	2.0
Depth	0.9	Depth	1.5

and 14 cm. In case of Model B, the model tests were conducted at draft of 11 cm. Consequently, there was a 2 cm layer of water on top of the cofferdam.

Photographs and drawings of the plain moonpool and the models with different cofferdam geometries are shown in Figs. 6 and 7, respectively.

4 Wave condition and test conditions

The test conditions were selected to cover the piston-mode and sloshing-mode resonances of the models. At PNU, model tests were carried out under a motion-allowed condition and fixed condition. Regarding the motion-allowed condition, heave motion was only allowed during the tests. At Koje College, each model was tested under the fixed condition. Table 3 summarizes the test conditions for each model. The incident wave height for the model tests was 2 cm for all wave frequencies. Head-sea of 180° heading is defined as a longitudinal direction of the moonpool as shown in Fig. 5. The cofferdam is located rear of the moonpool with respect to the head-sea. Wave heading is defined to be in a counterclockwise direction.

5 Experimental results and analysis

Theoretical formulas proposed by Molin were used to predict the resonance frequencies of the piston-mode and sloshing-modes [8].

Theoretical formula for the piston-mode is

$$\omega_n = \sqrt{\frac{g}{h(1+C)}} \tag{1}$$

where, g is the acceleration of gravity, h is draft, and C can be written as Eq. 2

$$C = \frac{1}{2\pi}\cdot\frac{1}{blh}\left[b^2 l \arg\sinh\frac{l}{b} + bl^2 \arg\sinh\frac{b}{l} + \frac{1}{3}(b^3 + l^3) - \frac{1}{3}(b^2+l^2)^{3/2}\right] \tag{2}$$

Theoretical formula for the sloshing-mode is

$$\omega_n \simeq \sqrt{g\lambda_n \frac{1 + J_n \tanh(\lambda_n h)}{J_n + \tanh(\lambda_n h)}} \tag{3}$$

where, $\lambda_n = \frac{n\pi}{l}$ and J_n can be written as Eq. 4.

$$J_n = \frac{2}{n\pi^2 r}\left\{\int_0^1 \frac{r^2}{u^2\sqrt{u^2+r^2}}\left(1 + (u-1)\cos(n\pi u) - \frac{\sin(n\pi u)}{n\pi}\right)du + \frac{1}{\sin\theta_0} - 1\right\} \tag{4}$$

with $r = \frac{b}{l}$ and $\tan\theta_0 = \frac{1}{r}$.

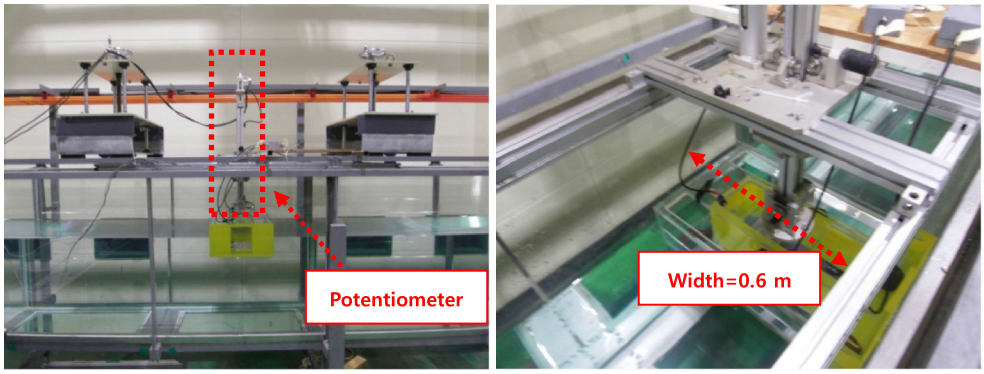

Fig. 3 2D wave flume at Pusan National University (*left*) and potentiometer for motion measurement (*right*)

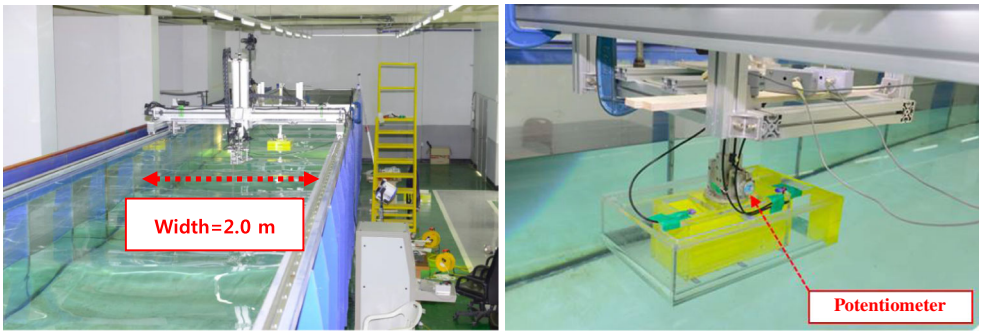

Fig. 4 2D wave flume at Koje College (*left*) and potentiometer for motion measurement (*right*)

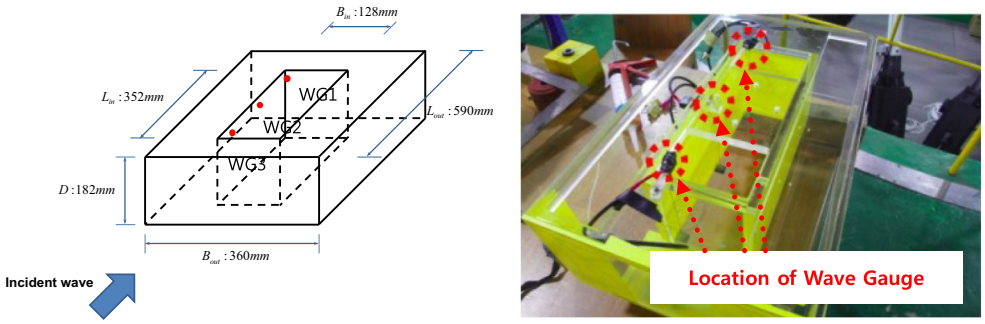

Fig. 5 Dimensions of barge-type vessel model with a moonpool (Model B) and locations of wave gauges

Table 2 Main dimensions of test models

Model B		Moonpool	
L (model length)	590 mm	l (moonpool length)	352 mm
B (model breadth)	360 mm	b (moonpool breadth)	128 mm
D (model depth)	182 mm	d (moonpool depth)	182 mm
Displacement (draft = 110 mm)	18,407,840 mm^3	–	–
Displacement (draft = 140 mm)	23,428,160 mm^3	–	–

The theoretical formulas for the resonance frequencies of each mode are based on single mode approximations under assumptions where the barge with infinite length and beam is motionless. As a result, the piston-mode resonance frequency for the infinite size of the barge could be slightly different. However, the effect of infinite size of the barge was not investigated in his work.

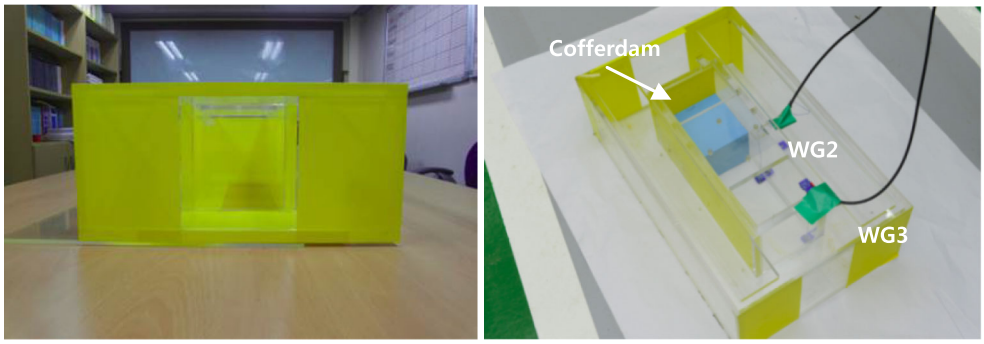

(a) Model B **(b)** Model Bc

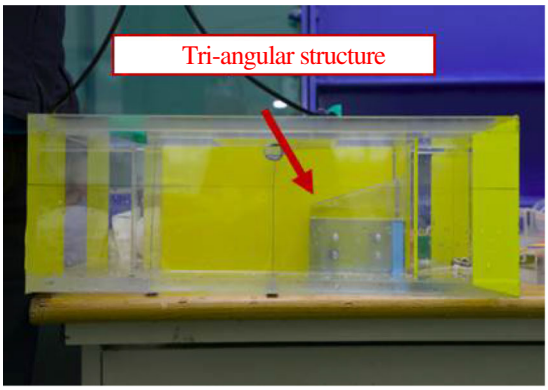

(c) Model Bc_tri

Fig. 6 Photographs of test models

Wave gauge relative water elevation (WG RWE) and motion response amplitude operator (RAO) are defined as follows:

WG RWE	Motion RAO
Relative water elevation in a moonpool/incident wave	Heave motion of a vessel/ incident wave

The wave gauges measured the relative water elevations inside the moonpool. The relative water elevation inside the moonpool refers to the distance from the baseline of the model to the free surface.

5.1 Sample time history of measured data

Figure 8 through Fig. 9 show samples of time histories of the measured data. Figure 8 presents the time history of an incident wave. Figure 9 presents the time histories of WG1 RWE ~ WG3 RWE and fast Fourier transform (FFT) results. Figure 10 presents the time histories of WG1 RWE ~ WG3 RWE, time history of the heave motion, and FFT results of the measured data. In particular, the incident wave was reflected and diffracted by the vessel model in the 2D wave flume. Therefore, the wave data without the model in the wave flume were used for the data analysis.

The sample time histories are the test results for an incident wave of 1.10 Hz. The test results present some differences between the fixed condition and motion-allowed condition. For the same incident wave, the WG amplitudes for the fixed condition were about 2.5 times higher than the motion-allowed condition. The wave energy was split into the vessel model and the flow in the moonpool in case of the motion-allowed condition whereas all of the wave energy was converted into the flow in the moonpool in case of the motion-fixed condition. Therefore, the relative water elevation in the moonpool for the motion-fixed condition was higher than that for the motion-free condition.

Based on the results of the model tests, all of the time histories were summarized at each frequency as depicted in terms of WG RWE and motion RAOs.

5.2 Piston-mode resonance for a plain moonpool

The piston-mode resonance for Model B is clearly observed as shown in Fig. 11. The height of the water

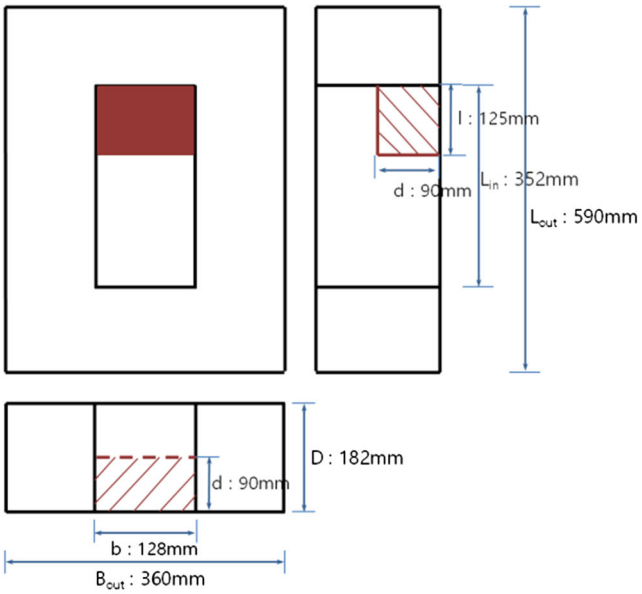

(a) Model Bc (Model B + cofferdam)

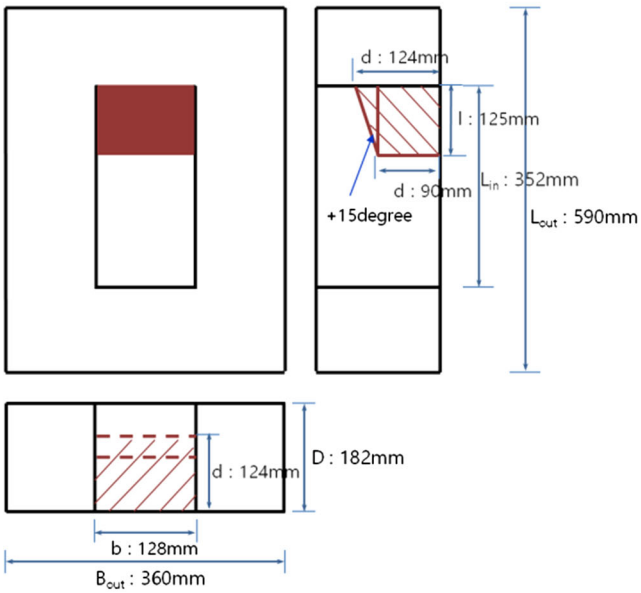

(b) Model Bc tri (facing left:+15deg)

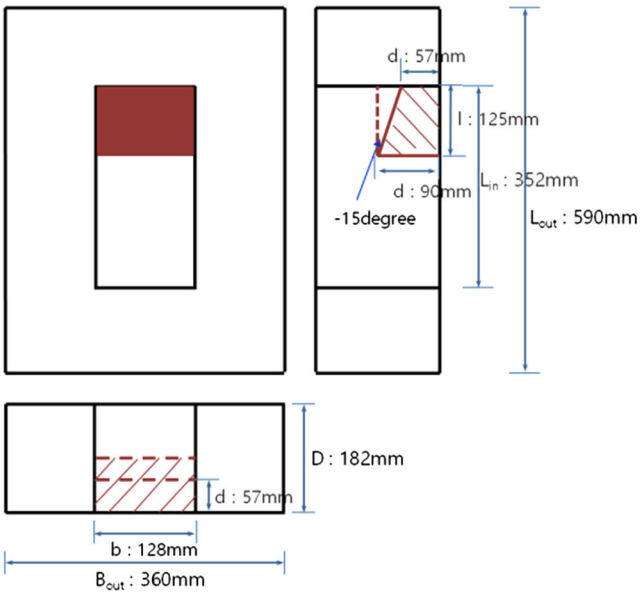

(c) Model Bc tri (facing right:-15deg)

Fig. 7 Drawings of test models

Table 3 Test conditions for model tests

Model name.	Test condition	DOF	Remark
Model B	Motion-allowed	Heave	3D model
	Fixed	–	
Model Bc	Motion-allowed	Heave	3D model with cofferdam
	Fixed	–	
Model Bc_tri	Motion-allowed	Heave	3D model with cofferdam + triangular structure
	Fixed	–	

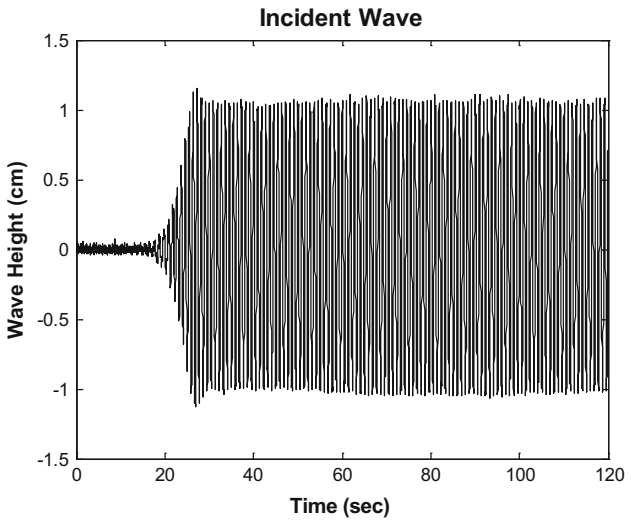

Fig. 8 Time history of incident wave

column inside the moonpool was much larger than that of the incoming wave. The measured piston-mode resonance frequencies for all of the tests are summarized in Table 4. Relative water elevations were relatively high near the resonance frequency whereas the relatively low far from the resonance frequency as shown in Figs. 12 and 13.

Very similar flow responses in the moonpool for full range of wave frequencies were observed between PNU and Koje College for Model B at draft of 11 cm. As summarized in Table 4, the measured resonance frequencies in PNU and Koje College model tests were 1.12 and 1.18 Hz, respectively. The small discrepancy in resonance frequency between model test results and the theoretical value might come from the experimental errors in, such as, data signal processing. Also, in Molin's theoretical formula, the model is assumed to be motionless and infinitely long and wide. The assumption in Molin's theoretical formula was not applied to the model tests with model of the finite size.

In case of motion-allowed condition at PNU, the measured resonance frequency was slightly higher than that at Koje College. The shift of the resonance frequency into higher frequency region was observed at both drafts of 11 and 14 cm. This goes along with the discrepancy from Molin's theoretical approach as both Molin's theory and model test at Koje College were motionless, or fixed. Although there was small discrepancy in resonance frequencies, the model tests strongly supported Molin's theoretical approach.

The moonpool resonance frequencies of the models were determined by their moonpool geometries. In the resonance point of view, different wave direction is not important. However, there is a possibility to affect the relative water elevation in the moonpool by different wave direction. According to the study of Maisondieu et al. [7], model test results of well head barge presented different relative water elevations in the moonpool for three different wave headings. In this regard, the investigations of flow responses inside the moonpool for different wave headings are necessary. To investigate the magnitude of the relative water elevation in the moonpool for different wave directions, model tests at head-sea and beam-sea were carried out. Figure 12 presents a comparison of the WG RWE and heave RAO of Model B for the head-sea condition and beam-sea condition. The piston-mode resonance frequencies under the head-sea and beam-sea conditions were the same in the model tests. The relative water elevations in the moonpool were similar under both head-sea and beam-sea conditions for most of the frequencies, except for frequencies near the resonance frequency. Higher relative water elevations in the moonpool were observed under the head-sea condition than the beam-sea condition near the resonance frequency. Particularly, the WG RWE at resonance frequency under the head-sea condition came out to be 48.3 % larger than that under the beam-sea condition.

Slightly larger heave motion was observed under the beam-sea condition than the head-sea condition in the low frequency region, under 0.9 Hz. A slight drop in heave motion at the piston-mode resonance frequency was observed in the model tests. Further study will be conducted on the drop of heave motion.

The model tests at draft of 14 cm were performed as well. Figure 13 shows the comparison of the relative water elevation and heave RAOs between the model tests at drafts of 11 and 14 cm. As shown in Fig. 13, the piston-mode moonpool resonance frequency at deeper draft had a lower frequency. The test at draft of 14 cm resulted 22.1 % higher WG RWE compared to that at draft of 11 cm. However, the test results at draft of 14 cm show slightly smaller RAO amplitude than that at draft of 11 cm for heave motion. In case of draft of 14 cm, the heave RAO near the resonance frequency (1.10 Hz) also showed the slight drop as well.

5.3 Flows inside a moonpool with cofferdam

Figure 14 presents the relative water elevations inside the moonpool for the plain moonpool and moonpool with the cofferdam under the beam-sea condition. From the model test results, the presence of the cofferdam influenced the resonance frequency and flow in the moonpool. In case of Model Bc, a second peak was observed in low frequency region far from the resonance frequency in both tests at PNU and Koje College (Figs. 14 and 15). Also, the cofferdam generated a transverse wave inside the moonpool under the beam-sea condition, as shown in Fig. 16. Furthermore, it was observed that the wave generated inside

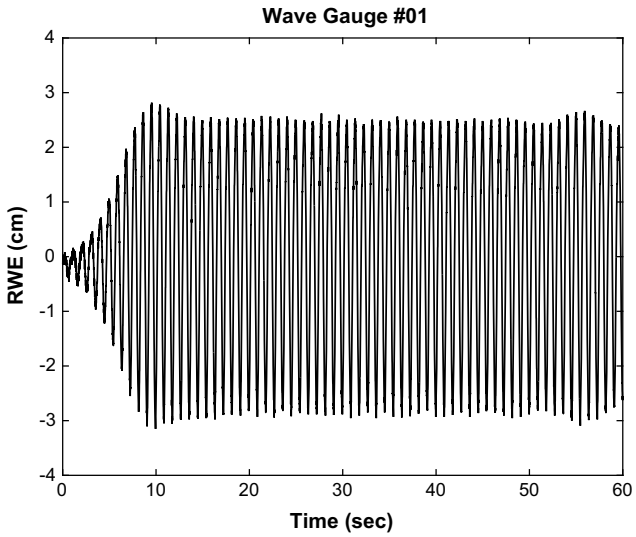

(a) Time history of wave gauge #01

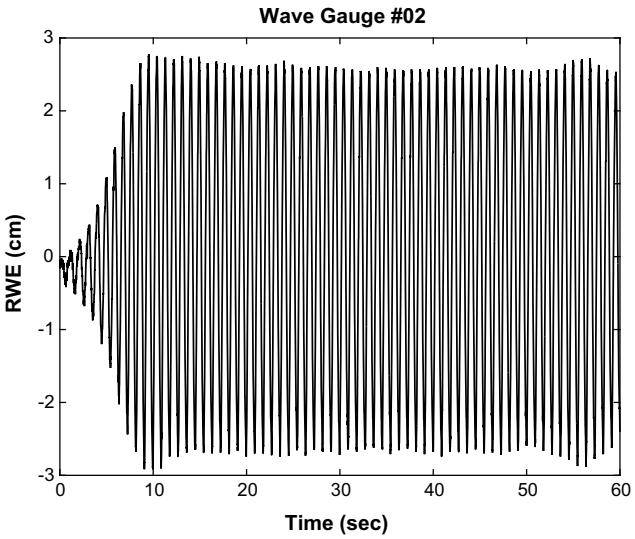

(b) Time history of wave gauge #02

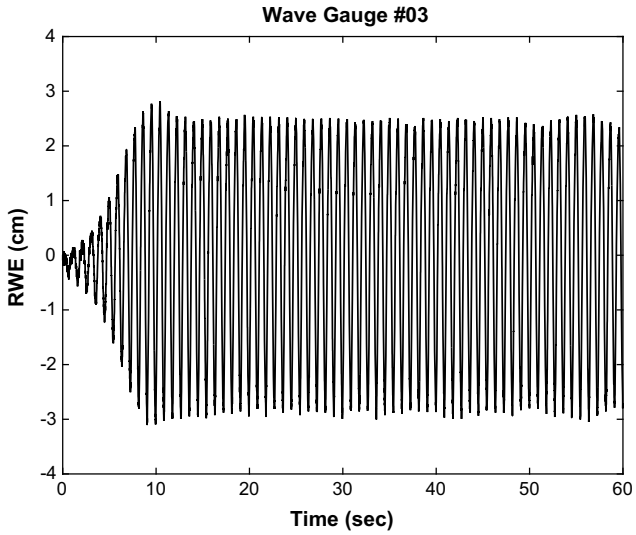

(c) Time history of wave gauge #03

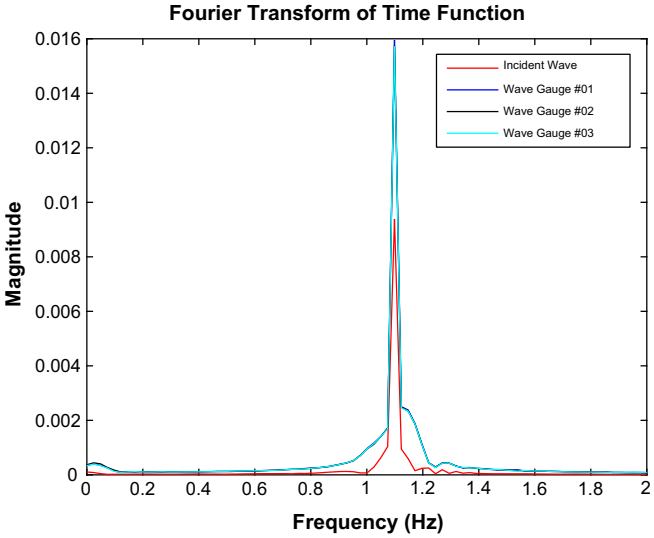

(d) FFT of measured data

Fig. 9 Measured data for fixed condition

the moonpool was reflected from the wall and propagated to the opposite wall in the transverse direction. As the propagation of waves was repeated, the relative elevation inside the moonpool was magnified (Fig. 17).

Figure 15 shows the WG RWE in the moonpool for the model with the cofferdam (Model Bc). In contrast to the plain moonpool (Model B), the model with the cofferdam presented three peaks under the head-sea condition. In particular, WG3 RWE located near the wall, had the highest value at 1.30 Hz. Similarly, in case of the moonpool with the cofferdam (Model Bc), the ascent and descent of the water column was transformed into sloshing wave. The generated sloshing wave was reflected from the moonpool wall and continuously amplified. The amplified sloshing wave caused splashing in the moonpool observed in the model test. Such splashing in the moonpool may not ensure the safety of workers under some real-sea conditions.

5.4 Comparison of model test results for different wave flume widths: wall effect on WG RWE inside a moonpool

The 2D wave flume at Koje College is about three times wider than the 2D wave flume at PNU. The model test for the fixed condition at PNU was carried out under beam-sea condition. However, the model test for the fixed condition at Koje College was performed under head-sea and

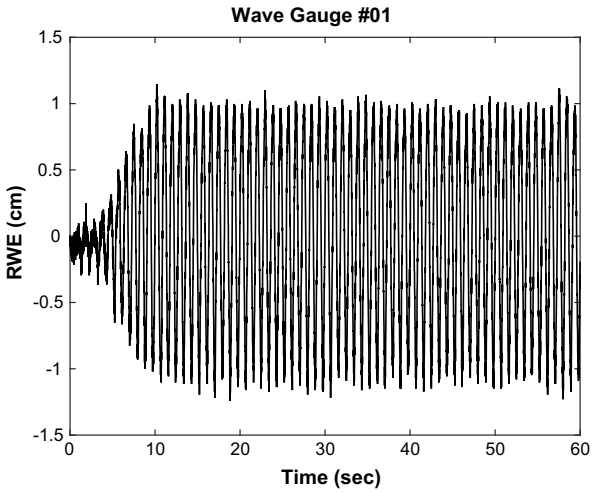

(a) Time history of wave gauge #01

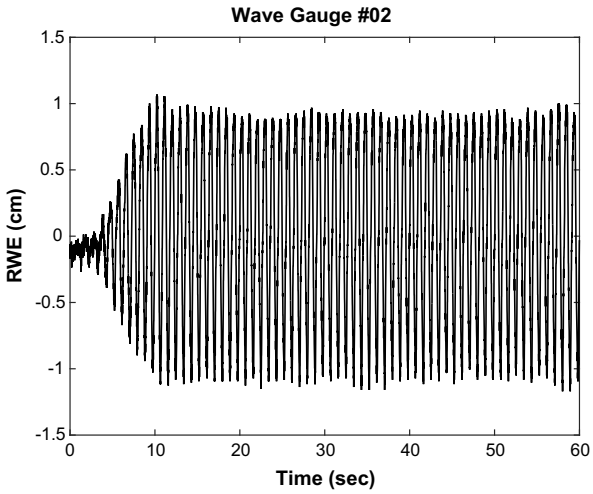

(b) Time history of wave gauge #02

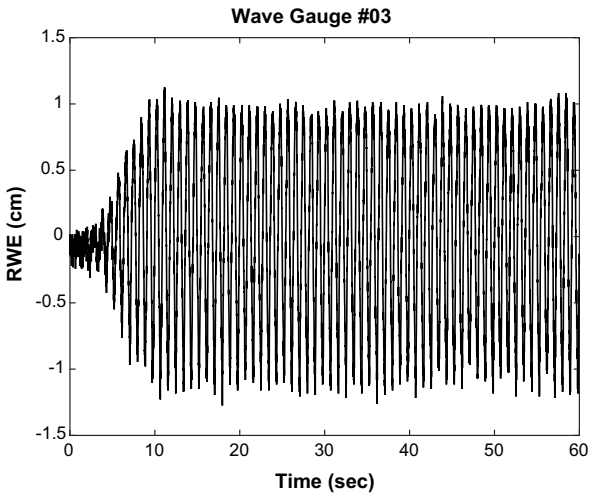

(c) Time history of wave gauge #03

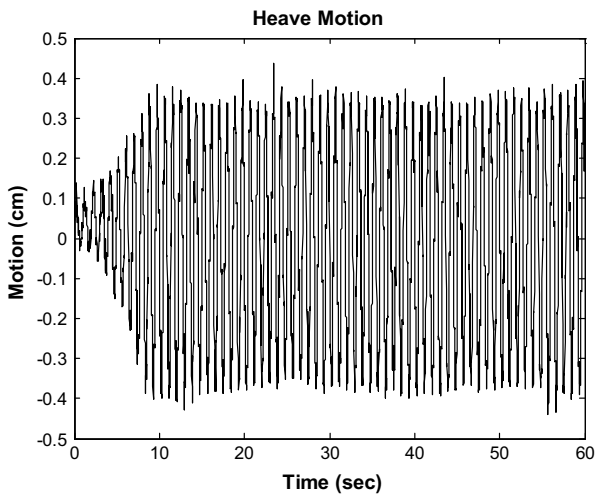

(d) Time history of heave motion

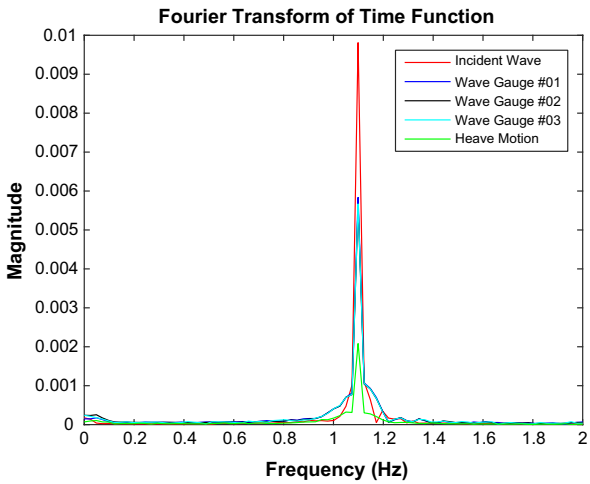

(e) FFT of measured data

Fig. 10 Measured data for motion-allowed condition

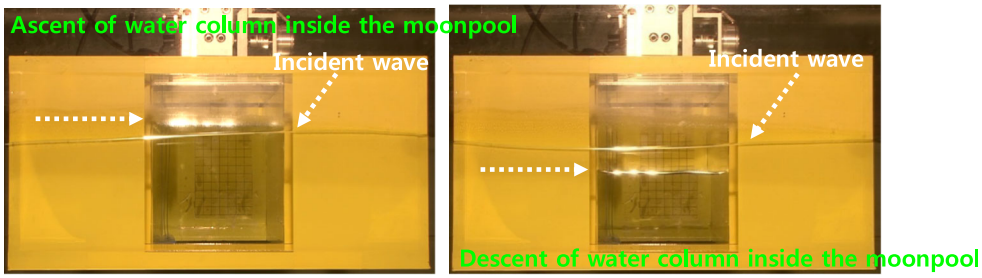

Fig. 11 RWE at piston-mode resonance frequency for fixed condition (model B)

Table 4 Summary of piston-mode moonpool resonance frequencies

Model	Draft (cm)	Test condition	Heading	Model test (Hz)	Molin's formula (Hz)	Facility
Model B	11	Motion-allowed	Head-sea	1.20	–	PNU
			Beam-sea	1.20		PNU
		Fixed	Head-sea	1.18	1.10	Koje College
			Beam-sea	1.12		PNU
	14	Motion-allowed	Head-sea	1.10	–	PNU
		Fixed	–	–	1.03	–
Model Bc	11	Motion-allowed	Beam-sea	1.30	–	PNU
		Fixed	Head-sea	1.30	–	Koje College
			Beam-sea	1.30		PNU

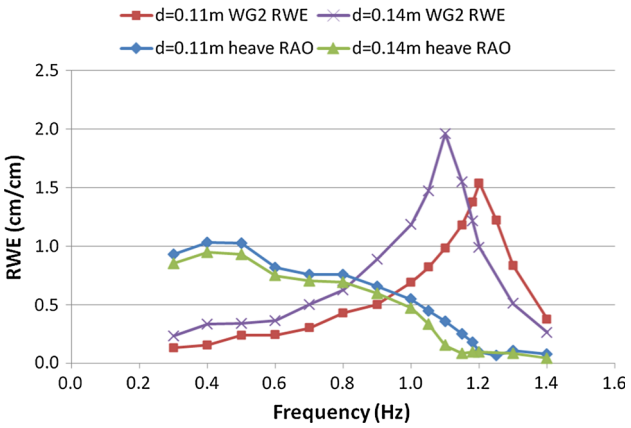

Fig. 13 Comparison of RWE values inside moonpool between 11-cm draft and 14-cm draft for motion-allowed condition (Model B)

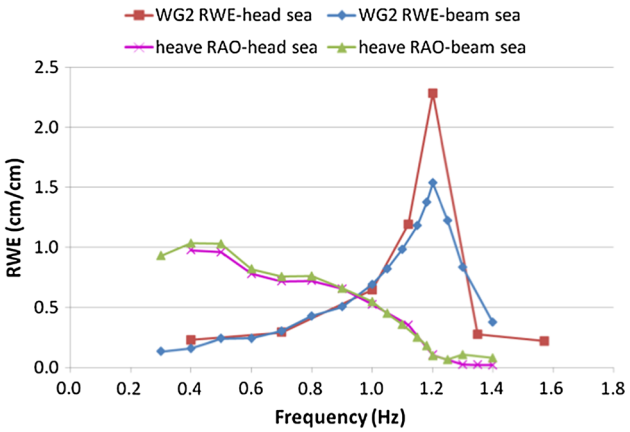

Fig. 12 Comparison of RWE and heave RAO between head-sea and beam-sea for motion-allowed condition (Model B)

quartering-sea condition. Even though the headings were different for two wave flumes, the effects of their different widths could be analyzed. The smaller width wave flume at PNU had higher WG RWE values at most frequencies except for the low frequency region under 0.4 Hz. The WG RWE values were almost the same in the low frequency region under 0.4 Hz. It is presumed that the wave energy escaped to the side of the model in the Koje College model test. Hence, it is concluded that the wider width presented a lower relative water elevation in the moonpool.

5.5 Sloshing-mode resonance for a plain moonpool

Another important resonance mode in a moonpool is the sloshing-mode Fig. 18 shows the generated wave elevation for the sloshing-mode under head-sea condition. The sloshing-mode resonance occurred at 1.57 Hz. The measured resonance frequency exactly matched to the theoretical resonance frequency. It turned out to be that the sloshing-mode resonance frequency was 1.3 times of the piston-mode resonance frequency. The relative water

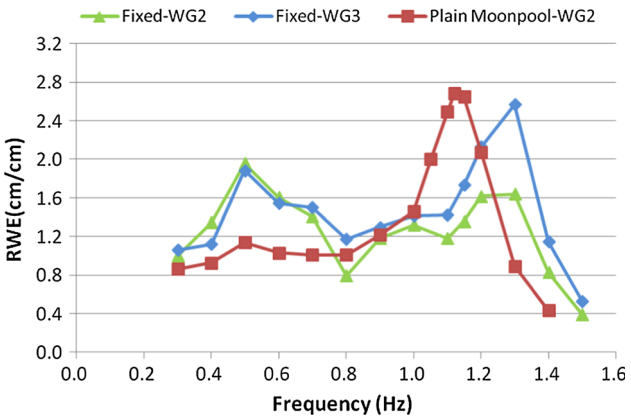

Fig. 14 Comparison of RWE values between plain moonpool and Model Bc under the beam-sea condition for fixed condition (PNU model test)

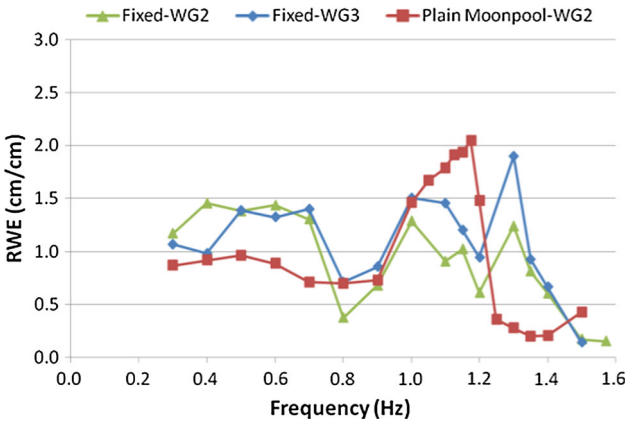

Fig. 15 Comparison of RWE values between plain moonpool and Model Bc under the head-sea for fixed condition (Koje College model test)

elevation measurements at each WG were different during the sloshing mode. If it were the piston-mode, the relative water elevation measurements would be the same for all WGs. At sloshing-mode resonance frequency, measured WG1 RWE and WG3 RWE were higher than measured WG2 RWE located in the center of the moonpool.

Unlike the PNU model test, it was possible to perform an oblique test in the 2D wave flume at Koje College for the wider wave flume as shown in Fig. 19. The resonance frequencies were observed to be almost the same as summarized in Table 5. For the motion-allowed condition in the PNU model tests, the sloshing-mode resonance was found at 1.57 Hz. For the fixed condition in Koje college model tests, the sloshing-mode resonance frequencies were at 1.60 Hz under head-sea condition and 1.57 Hz under quartering-sea condition. Very small discrepancy of 0.03 Hz might fall into model test error range or come from experimental errors of data signal processing. Figure 20 shows the water moving up in bow and stern side walls for the sloshing-mode under the quartering-sea condition (heading of 45°).

The model test results under head-sea and quartering-sea for the fixed condition in the wave flume at the Koje College were compared. The relative water elevations in the moonpool for the sloshing-mode resonance under a quartering-sea condition were higher than that under beam-sea as shown in Fig. 21. Difference in the relative water elevations in the moonpool for the sloshing-mode resonance between quartering-sea and beam-sea should be further investigated through wider scope of model test and numerical calculations.

5.6 New design of inner structure to reduce violent flow in a moonpool

To reduce the relative water elevation inside the moonpool, two different right triangle structures were attached to the top of the cofferdam. One right triangle structure facing right and another facing left were installed as shown in Fig. 22a and b, respectively.

The test model with the right triangle structure facing left reduced the height of the sloshing wave in the moonpool by acting as a beach (Fig. 23) whereas the test model facing right did not reduce the flow inside the moonpool as presented in Fig. 24. For the model facing left, WG RWEs in the moonpool were lower over the entire range of wave frequency. However, WG RWEs in the moonpool with the model facing right were relatively higher, especially near the resonance frequency. It was observed that a violent flow was generated inside the moonpool because the vertical side of the right triangle faced to the right.

6 Conclusions

An experimental study on the piston-mode and sloshing-mode moonpool resonances was presented. To investigate the efficiency of different cofferdam geometries, three models were tested. Different wave directions were considered to investigate the relative water elevation in the moonpool in relation to the wave directions.

The following conclusions are drawn from the present study:

1. The model with the right triangle facing left on the top of the cofferdam was the most effective in reducing the flow in the moonpool from the model test results.

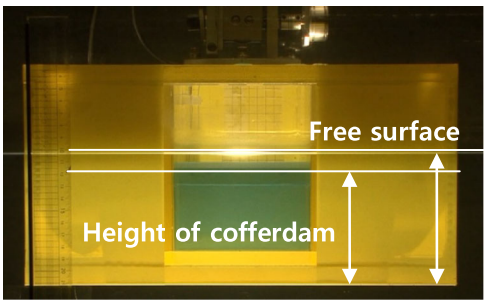

(a) Initial calm sea state

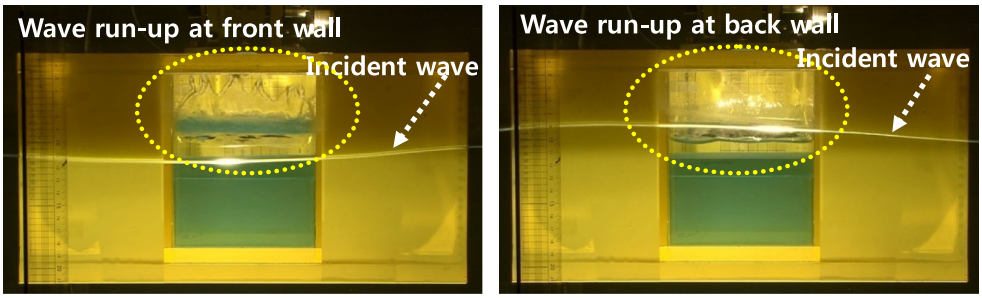

(b) During model test

Fig. 16 RWE at 1.30 Hz resonance frequency for fixed condition (Model Bc)

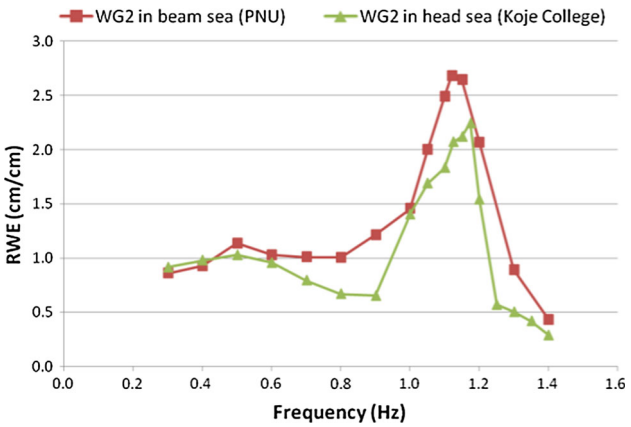

Fig. 17 Comparison of RWE values between model test results at PNU and Koje College under fixed conditions

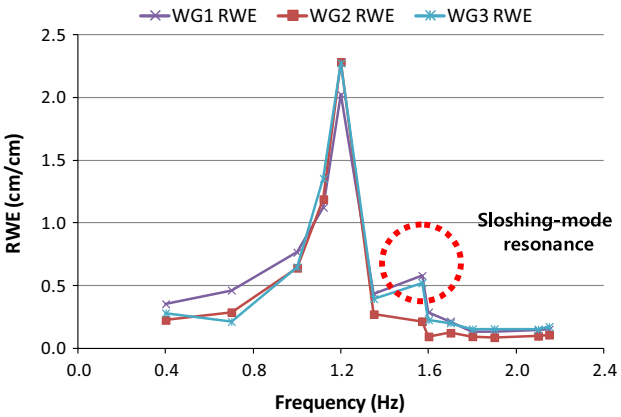

Fig. 18 RWE inside the moonpool under a head-sea condition for the motion-allowed condition

2. The model with the right triangle facing right on the top of the cofferdam magnified the flow in the moonpool at three frequencies.
3. Placing a cofferdam in the moonpool caused violent sloshing waves instead of ascent and descent of the water column in the piston-mode resonance.
4. The installation of the cofferdam generated additional peaks under head-sea for the fixed condition in addition to the primary peak at the moonpool resonance frequency. The longitudinal travelling waves caused the additional peaks.

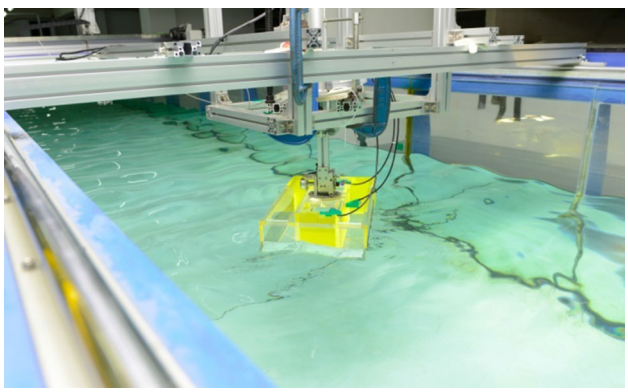

Fig. 19 Model test under quartering-sea condition in the 2D wave flume in Koje College

Table 5 Summary of sloshing-mode moonpool resonance frequencies

Model	Test condition	Heading	Model test (Hz)	Molin's formula (Hz)	Facility
Model B	Motion-allowed	Head-sea	1.57	–	PNU
	Fixed	Head-sea	1.60	1.57	Koje College
		Quartering-sea	1.57	–	Koje College

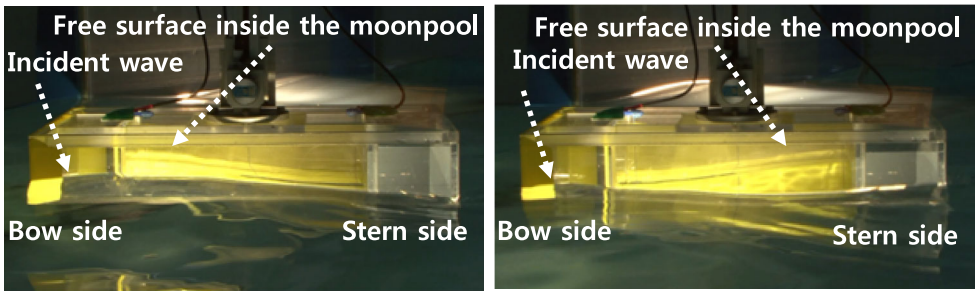

Fig. 20 Water moving up in bow side wall (*left*) and in stern side wall (*right*) for sloshing-mode at the quartering-sea (heading of 45°)

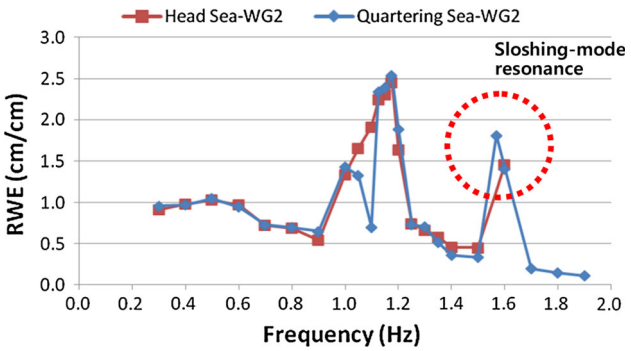

Fig. 21 Comparison of RWE values between the head-sea and quartering-sea for fixed condition (Model Bc)

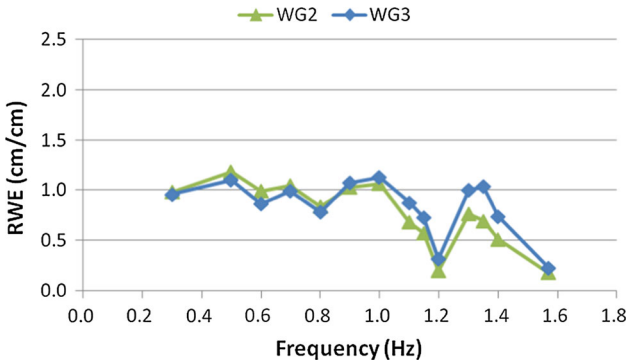

Fig. 23 RWE for model with *right triangle facing left on top* of the cofferdam

5. Flow responses in the moonpool in two wave flumes with different widths gave very similar results across full range of frequency.
6. The wave flume width indeed influenced the relative water elevation in the moonpool as wider wave flume produced lower relative water elevation in the moonpool.
7. Molin's theoretical formula was accurate to predict the resonance frequencies of the piston- and sloshing-

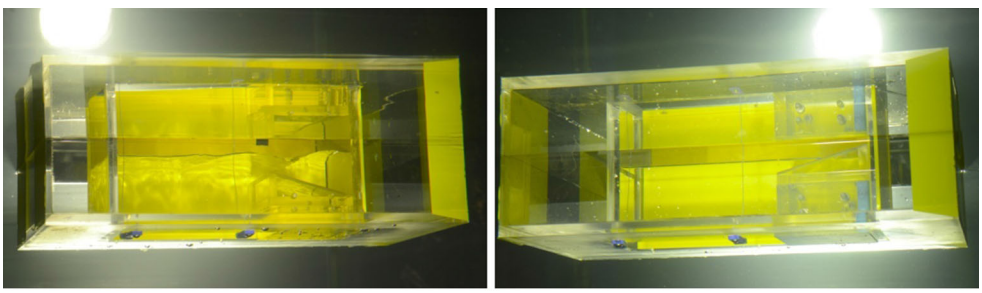

(a) Right triangle facing right **(b)** Right triangle facing left

Fig. 22 Models with *different triangle* structures on *top* of the cofferdam

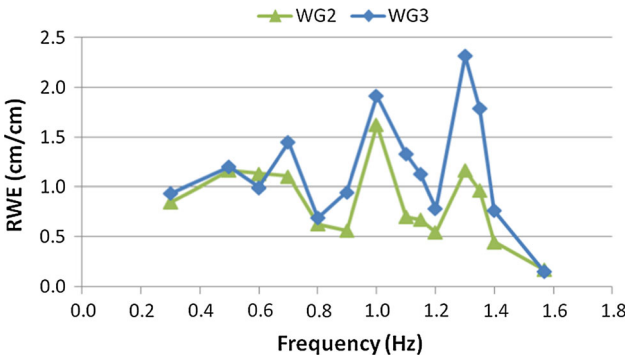

Fig. 24 RWE for model with *right triangle facing right on top* of the cofferdam

modes even though it was derived under the assumption of fixed body and infinite size of the barge.

8. WG RWE values inside the moonpool in the piston-mode resonance were higher under the head-sea condition than under the beam-sea condition.
9. WG RWE values inside the moonpool in the sloshing-mode resonance were higher under the quartering-sea condition than under the head-sea condition.

Acknowledgments This work was supported by a National Research Foundation of Korea (NRF) Grant funded by the Korea government (MSIP) through GCRC-SOP (No. 2011-0030013).

References

1. Choi SY, Lee YG, Jung KY (2010) A fundamental study for internal flow in moonpool using marker-density method by two-dimensional numerical simulation. Spring Conference of the Society of Naval Architects of Korea, Jeju, Korea
2. Choi SY, Lee YG, Jung KY (2011) Reduction of added resistance by internal flow control in the moonpool of a drillship. J Soc of Nav Archit Korea 48:544–551
3. Hammargren E, Tőrnblom J (2012) Effect of the moonpool on the total resistance of a drillship. Chalmers University of Technology. MSc Thesis
4. Fukuda K (1977) Behavior of water in vertical well with bottom opening of ship, and its effects ship-motion. J Soc of Nav Archit Korea 141:107–122
5. Gaillarde G, Cotteleer A (2004) Water motion in moonpools empirical and theoretical approach. ATMA (Association Technique Maritime et Aeronautique), Paris
6. Han SY, Ha MK (2002) Ultra deepwater drillship. J Nav Archit Ocean Eng, 39(2)
7. Maisondieu C and Ferrant P (2003) Evaluation of the 3D flow dynamics in a moonpool. In: Proceedings of the Thirteenth International Offshore and Polar Engineering Conference, Honolulu, Hawaii, USA, 25–30 May, 2003
8. Molin B (2001) On the piston and sloshing modes in moonpools. J Fluid Mech 430:27–50
9. Park SJ (2009) Hydrodynamic characteristics of moonpool shapes. Pusan National University. MSc Thesis
10. Veer, R. and Tholen, H. J. (2008) Added resistance of moonpools in calm water. Proceedings of the ASME 27th International Conference on Offshore Mechanics and Arctic Engineering, Estoril, Portugal, 15–20 June 2008
11. Yang SH, Kwon SH (2013) Experimental study on moonpool resonance of offshore floating structure. J Nav Archit Ocean Eng 5:313–323
12. Yang SH, Yang YJ, Lee SB, Do JT, Kwon SH (2013) Study on the moonpool resonance effect to the motion of a modern compact drillship. J Korea Soc Ocean Eng 27(3):53–60
13. Yeom DJ (2010) Dynamics of marine structures, 1st edn. Ulsan University, Ulsan
14. You KH, Jung SH, Das PK (2008) Improved construction method for modern drillships, Offshore Technology Conference, Houston, USA